Class 4 Active RFID Multi-hop Relay System based on IEEE 802.15.4a Low-Rate UWB in Sensor Network

Hong Zhang, SungHyun Hong and KyungHi Chang
The Graduate School of Information Technology and Telecommunications, INHA University
Incheon 402-751, Korea
[e-mail: zhanghong.email@gmail.com, akaraba@naver.com, khchang@inha.ac.kr]

Abstract

The low-rate (LR) UWB is a promising technology for the ubiquitous sensor network (USN) due to its extremely low power consumption and simple transceiver implementation. However the limited communication range is a bottleneck for its widespread use. This paper deals with a new frame structure of class 4 active RFID multi-hop relay system based on ISO/IEC 18000-7 standard integrating with IEEE 802.15.4a LR-UWB PHY layer specification, which sets up a connection to USN. As a result of the vital importance of the coverage and throughput in the application of USN, further we analyze the performance of the proposed system considered both impulse radio UWB (IR-UWB) and chirp spread spectrum (CSS). Our simulation results show that the coverage and throughput are remarkably increased.

Keywords: LR-UWB, CSS, active RFID, multi-hop relay, USN

1. Introduction

Radio frequency identification (RFID) is rapidly developing for the coming ubiquitous sensor networks, in which class 4 active RFID [1] techniques enable the communications with near ad-hoc networks with battery assisted tags. The multi-hop relay system of active RFID has been proposed based on ISO/IEC 18000-7 specification, which will greatly enlarge the coverage of a sensor network [2][3].

Low-rate (LR) ultra-wide band (UWB) defined in IEEE 802.15.4a [4] is drawing more and more attentions in the applications active RFID and related fields, such as USN, due to its relatively low power consumption, complexity and high security (decreasing probability of interception). Also its higher time of arrival (TOA) resolution is a better choice for real time location system (RTLS). The rather small power spectral densities of UWB system guarantee only minimal mutual interference between the communications and a time hopping sequence is applied to against catastrophic collisions in multiple access [5][6].

However, the extremely short communication range restricts the effectiveness of UWB applied to RFID system. On the other hand, the collision problems in the dense RFID environment are remaining a critical bottleneck of large scale deployment of tags. In this paper, our purpose is to propose a frame structure of ISO/IEC 18000-7 active RFID based multi-hop relay system integrating with IEEE 802.15.4a LR-UWB PHY layer specification, which sets up a connection with the nearby sensor networks. Our proposed model turns out to be not only increasing the communication distance of LR-UWB based RFID system, but also raising the deployed number of tags in a given range.

The remaining part of this paper is organized as follows. The system model is first introduced in section 2 including IR-UWB, chirp spread spectrum (CSS), ISO 18000-7 active RFID specification, channel model and class 4 active RFID relay system. In section 3, a new frame structure is proposed. In section 4, the performance of throughput and coverage is evaluated and discussed. Finally, conclusions are given in section 5.

2. System Model of UWB based Multi-hop Relay System

2.1 IR-UWB

In IEEE 802.15.4a, the IR-UWB physical (PHY) layer defines three independent bands, sub-gigahertz (249.6-749.6 MHz), low band (3.1-4.8 GHz), and high band (6.0-10.6 GHz) including several channels of 500 MHz. A UWB impulse radio transmits a train of low duty cycle bursts. A single burst consists of N_{cpb} chips, whose amplitudes are modulated by a binary scrambling sequence. The N frames build up N bits transmitted signal and a frame is made up of N_c chips with T_c seconds. The position of the burst in the *kth* frame represents the *kth* bit information, which depends on the time hopping sequence, $N_{hop} = N_c / 4N_{hop}$. Thus the transmit signal is given by

$$S^{(k)}(t) = \sum_{k=-\infty}^{\infty} b_1^{(k)} p^{(k)}(t - b_0^{(k)}\Delta - h^{(k)}NT_c), \tag{1}$$

where $b_1^{(k)} \in \{\pm1\}$ and $b_0^{(k)} \in \{0,1\}$ are the *kth* (binary phase shift keying) BPSK and (binary position modulation) BPM data symbol. $p^{(k)}(t)$ is a burst with N_{cpb} chips. Δ is the BPM delay. $h^{(k)}$ is the time hopping code of integer chosen in $\{0, 1, \ldots, N_{hop}\text{-}1\}$. Both the scrambling

sequence and time hopping sequence are generated by a linear feedback shift register (LSFR) described in the IEEE 802.15.4a specification [7][8][9].

The parameters of N_{cpb}, N_{hop}, N_c, and T_c used in this paper are given in **Table 1** compliant with 802.15.4a PHY layer specification in [4]. The mandatory data rate of 0.87 Mbit/s (we consider the case with Reed-Solomon (RS) code only) is adopted with the mean pulse-repetition frequency (MPRF) 3.90 MHz.

Table 1. Parameters of IR-UWB PHY layer

N_{cpb}	N_{hop}	N_c	T_c (ns)	Bit Rate (Mb/s)	Mean PRF (MHz)
4	32	512	2	0.87	3.90

2.2 Chirp Spread Spectrum

In IEEE 802.15.4a CSS PHY layer, the operating frequency is 2.45 GHz. Each chirp symbol consists of four subchirps combined with differential quadrature phase-shift keying (DQPSK) and 8-ary coding for 1 Mb/s data rate. By using alternating time gaps in conjunction with sequences of chirp signals (subchirps) in different frequency subbands with different chirp directions, the CSS PHY provides subchirp sequence division as well as frequency division [10].

The time-domain base-band signal can be defined as

$$C^m(t) = \sum_{n=0}^{\infty} \sum_{k=1}^{4} C_{n,k} \exp\left[jT\left(2\pi f_{k,n} + \frac{\mu}{2}\xi_{k,m} \right) \right] \times P_{RC}(T), \tag{2}$$

where $m = 1, 2, 3, 4$ defines which of the four different possible chirp symbols (subchirp sequences) is used and $n = 0, 1, 2...$ is the sequence number of the chirp symbols. $k = m$ is the subchirp index. $C_{n,k}$ is the sequence of the complex data that consists of in-phase data and quadrature-phase data as the output of DQPSK coding. T defines the starting time of the actual subchirp signal to be generated. It is determined by T_{chirp}, which is the average duration of a chirp symbol, and by T_{sub}, which is the duration of a subchirp signal. The constant μ defines the characteristics of the subchirp signal. The function P_{RC} is a windowing function that is equal to zero at the edges and outside of the subchirp centered at time zero. **Table 2** lists the parameters we applied in simulation compliant with IEEE 802.15.4a CSS PHY layer described in [4].

Table 2. Parameters of CSS PHY Layer

Center Freq. (GHz)	T_{chirp} (μs)	T_{sub} (μs)	Bit Rate (Mb/s)
2.45	6	1.1875	1

2.3 ISO/IEC 18000-7 Active RFID Specification

In ISO/IEC 18000-7 active RFID specification, a frame structure is defined in **Fig. 1**, which is to perform an efficient and orderly collection of the tags placed within the interrogator (or namely reader) communication range. The interrogator is the master of the communication with one or multiple tags, while the tag transmissions are assigned into slots within specified collection round (or so called window size).

The tags move into *Ready* mode after receive "wake up" signal broadcasted by interrogator. Then a *Collection* command starts a collection round, which consists of a number of slots. Tags receiving a *Collection* command randomly select a slot to respond and wait for a

pseudo-random time delay equaling to the slot number multiplied by slot delay. The number of slots is determined by the current window size, indicated by the interrogator *Collection* command. Each slot is long enough for the interrogator to receive a tag response.
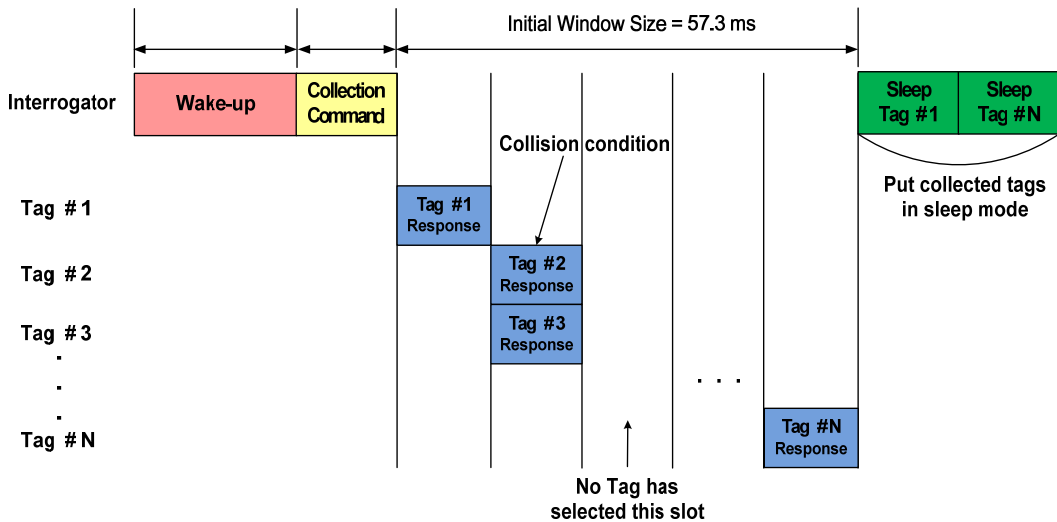
Fig. 1. Frame structure in ISO/IEC 18000-7.

The initial window size specified by the reader is given by

$$Window\ Size = Window\ Factor * 57.3\ ms, \tag{3}$$

where the window factor is an integer value used to change window size. It is fixed to 1 in the initial collection round and the minimum window size is set to 57.3ms. The interrogator records the received information via tag response, and counts the number of collisions in case of Tag #2 and Tag #3 in **Fig. 1**. The tags shall turn to *Sleep* mode after successful response and do not participate in the following collection rounds. The interrogator estimates the number of uncollected tags based on the counted collision numbers and determines the optimal window size for the next collection round by setting an appropriate window factor.

A slot size in ISO/IEC 18000-7 specification is defined as

$$Slot\ Size = Response\ Transmission\ Time + Slot\ Guard\ Time, \tag{4}$$

where response transmission time is around 1 ms for tags to transmit response packets. Slot guard time is fixed to 2 ms, which is the period that an interrogator deals with current receiving information and prepares for the next tag response. The number of slots is calculated by

$$Number\ of\ Slots = Window\ Size\ /\ Slot\ Size. \tag{5}$$

The interrogator immediately starts the next collection round by transmitting the *Collection* command. This process continues until no more tags are being detected during three subsequent collection rounds.

2.4 Class 4 RFID Multi-hop Relay System

The class 4 active RFID multi-hop relay system based on ISO/IEC 18000-7 active RFID specification can be simply described in the **Fig. 2** below. It is made up of a reader, several relay tags and a number of active tags.
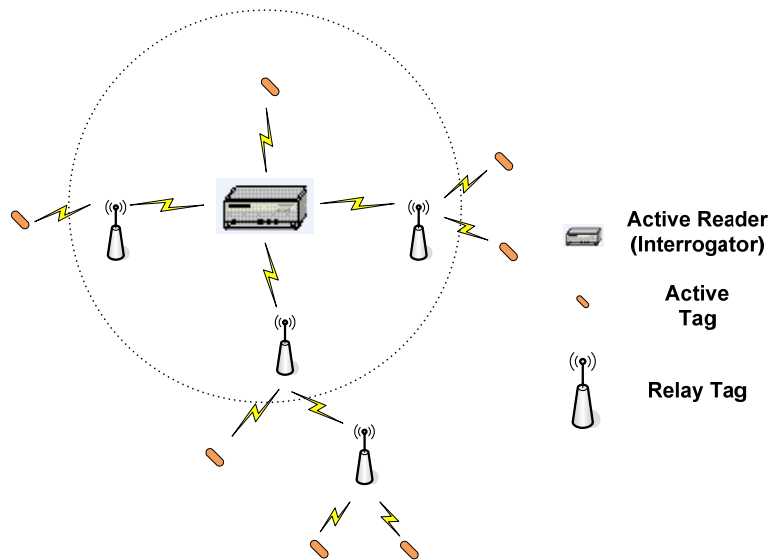

Fig. 2. Class 4 active RFID multi-hop relay system.

In the multi-hop scenario, first the reader broadcasts wake-up signal to both different types of tags in the coverage. The 1st relay tags, which have received signal, continue to send the same message to the 2-hop tags (the tags in the coverage of 1st relay tags). Step by step, the wake-up signal is delivered to the multi-hop end tags. Then all the tags, which have received the signal, move into ready state. In the second round, the reader initiates a tag collection process by sending a *Collection* command following the same way.

On receiving a *Collection* command, tags randomly select a slot in which to respond. The selection is determined by a pseudo-random number (PN) generator. When a tag selects a slot number it will wait for a pseudo-random time delay equal to a time of slot number multiplied by slot delay before it responds. The number of slots is determined by the current window size. Note here, the window size is fixed at first, after that the *Collision Arbitration* mode performs before the tags start transmitting. During the subsequent collision arbitration process, the reader dynamically chooses an optimum window size for the next collection round based on the number of collisions in the current round.

As **Fig. 3** shows the instance, in the first round the 2-hop tags will response to the 1st relay tags, and the message will temporally stored in the memory of 1st relay tags. Then in the second round, the 1st relay tags will deliver the message to the reader. The end tags will move into *Waiting* mode if they have collisions or *Sleep* mode if they finish successfully transmitting.

The active reader and the end tags are compliant with the ISO/IEC 18000-7 specification. Both 2-hop and 3-hop tags are normal class 4 active tags different with the relay tags, which shall play as a part role of reader and need higher power consumption, larger memory size and additional command modes.
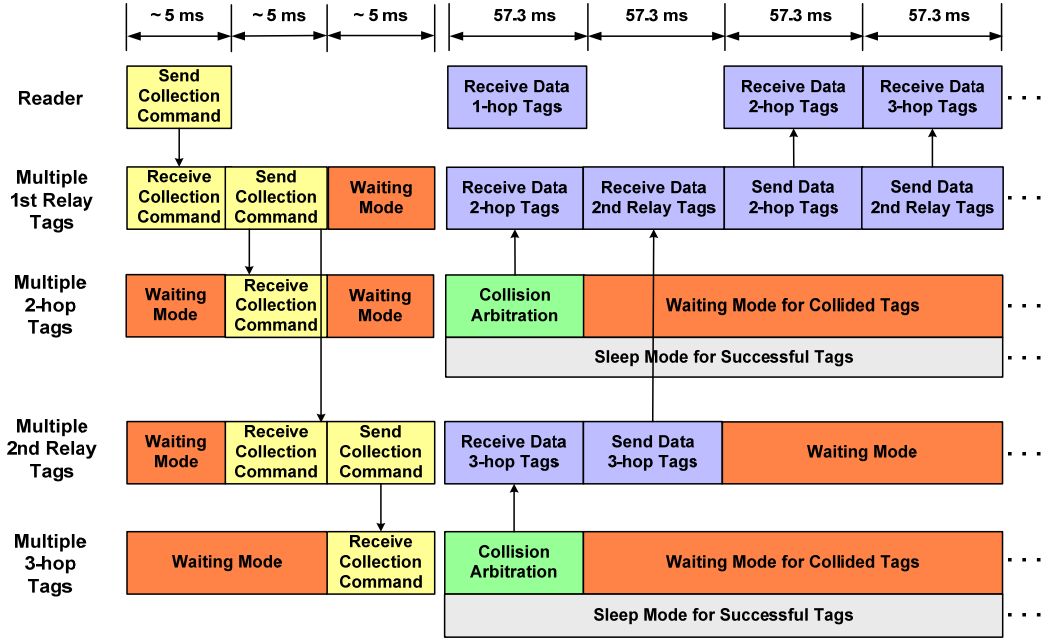
Fig. 3. Frame structure of 3-hop RFID relay system.

2.5   Channel Model for IEEE 802.15.4a UWB

The IEEE 802.15.4a UWB channel is modified SV-model, and defines nine sets of parameters for different environments using Nakagami-distribution for small-scale fading with different m-factors for different components. We use channel model 1 (CM1) in the simulation, which stands for indoor residential environment with line-of-sight (LOS) covering the frequency range from 2 to 10 GHz [11].

For large scale fading, the distance dependence of the pathloss model in dB scale is described by

$$PL(d) = PL_0 + 10n \log_{10}\left(\frac{d}{d_0}\right) + S, \tag{6}$$

where the reference distance d_0 is set to 1 m, and PL_0 is the pathloss at the reference distance. n is the pathloss exponent. The pathloss exponent also depends on the environment and on whether a LOS connection exists between the transmitter and receiver or not. Shadowing S is defined as the variation of the local mean around the pathloss, where S is a Gaussian-distributed random variable with zero mean and standard deviation σ_S. On considering AWGN scenario，the standard deviation σ_S is equal to 3.7 as the distance is tens of meters [12].

3. Proposed Low-Rate UWB based Class 4 Active RFID Multi-hop Relay System

In the proposed frame structure, we will first extend the active RFID multi-hop relay system to the ubiquitous sensor network. The information from local sensor networks as the tags for people and vehicles tracking, tags for traffic and pollution monitoring, and the container tags

in transportation can be forwarded by relay tags, collected by the central interrogator and transmitted to the database as **Fig. 4** shows. The proposed frame structure is remaining TDMA/TDD-half duplexing communication.
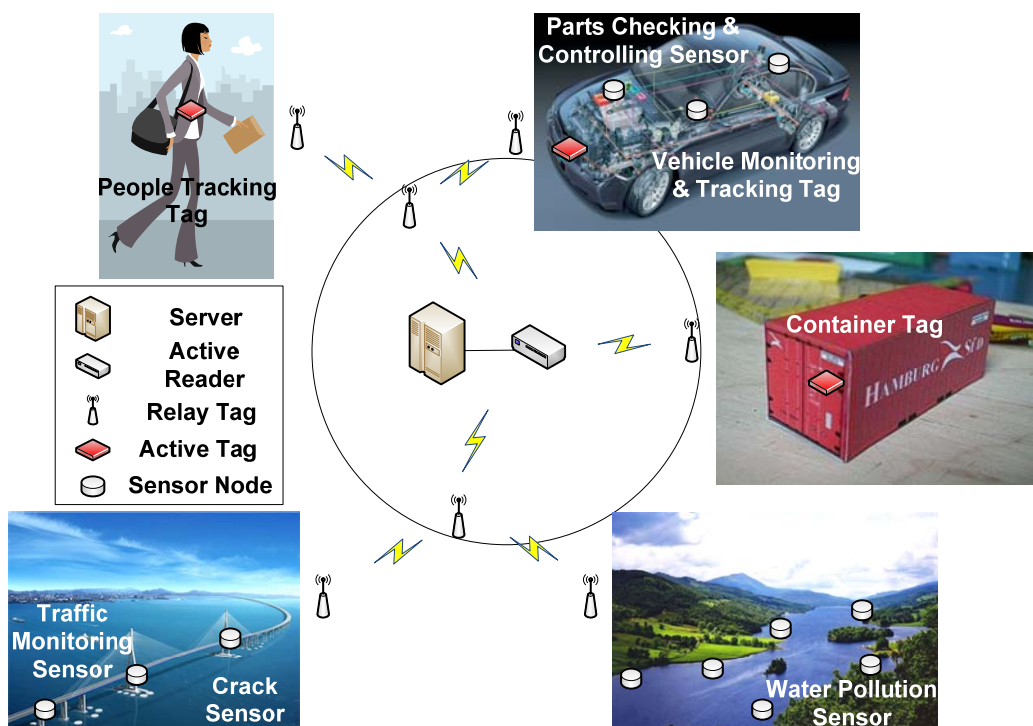

Fig. 4. Deployment scenario of the proposed class 4 RFID multi-hop relay system connected with USN.

We will take a 3-hop relay system for example with the scenario as **Fig. 5** shows: Single reader - Multiple relay tags - Multiple tags - Sensor nods. As previously mentioned, the reader broadcast the wake-up signal and Collection command to all the tags. The relay tags forward the signal to the end tags in the coverage hop by hop. At the same time, the relay tags are able to build a connection with the sensor nodes in the other local networks. For instance, the 2nd relay tags relay the command to the sensor nodes. Then the sensor nodes are activated and ready to communicate with the RFID relay system. Here we only consider the tags and sensor nodes based on LR-UWB technologies. All the sensors are compliant with IEEE 802.15.4a PHY layer specification.

A *Collision Arbitration* mode is performed in the collection round. Usually the mechanism is frame slotted aloha. In a frame, a tag is randomly assigned to a PN within the range of total time slots. A successful time slot means only one tag is interrogated in the current time slot. A time slot with collision stands for more than one tag are assigned to the same PN in order that they choose the same time slot, while an idle time slot has no tag to be interrogated. The tags in collision shall wait for the next frame and choose a PN again. The repeated frame process does not terminate until all the tags in the coverage are interrogated. After the tag is interrogated by the reader or a relay tag, it turns to *Waiting* mode until next collection round to be activated again.

However, the sensor nodes will perform a CSMA with copying collision avoidance (CSMA/CCA) mechanism to mitigate collisions different from the *Collision Arbitration* mode

of the active tags after the sensor nodes receive a *Collection* command. The CSMA/CCA copies the contention window (CW) size in the MAC header of an overheard data frame and updates its backoff counter according to the new CW size [13]. After the adaptable delay, they transmit the message to the 2nd relay tags. The collisions with the 3-hop tags are inevitable, thus the CW size should be calculated carefully considering all the tags and sensor nodes in the 2nd relay tags' coverage. When the reader completes collecting round, as existing active RFID system, it sends *Sleep* command to those tags, which have already sent message successfully in the current round. Then the tags will move into *Sleep* mode to save energy, and do not join the collecting round any more until they are reactivation.
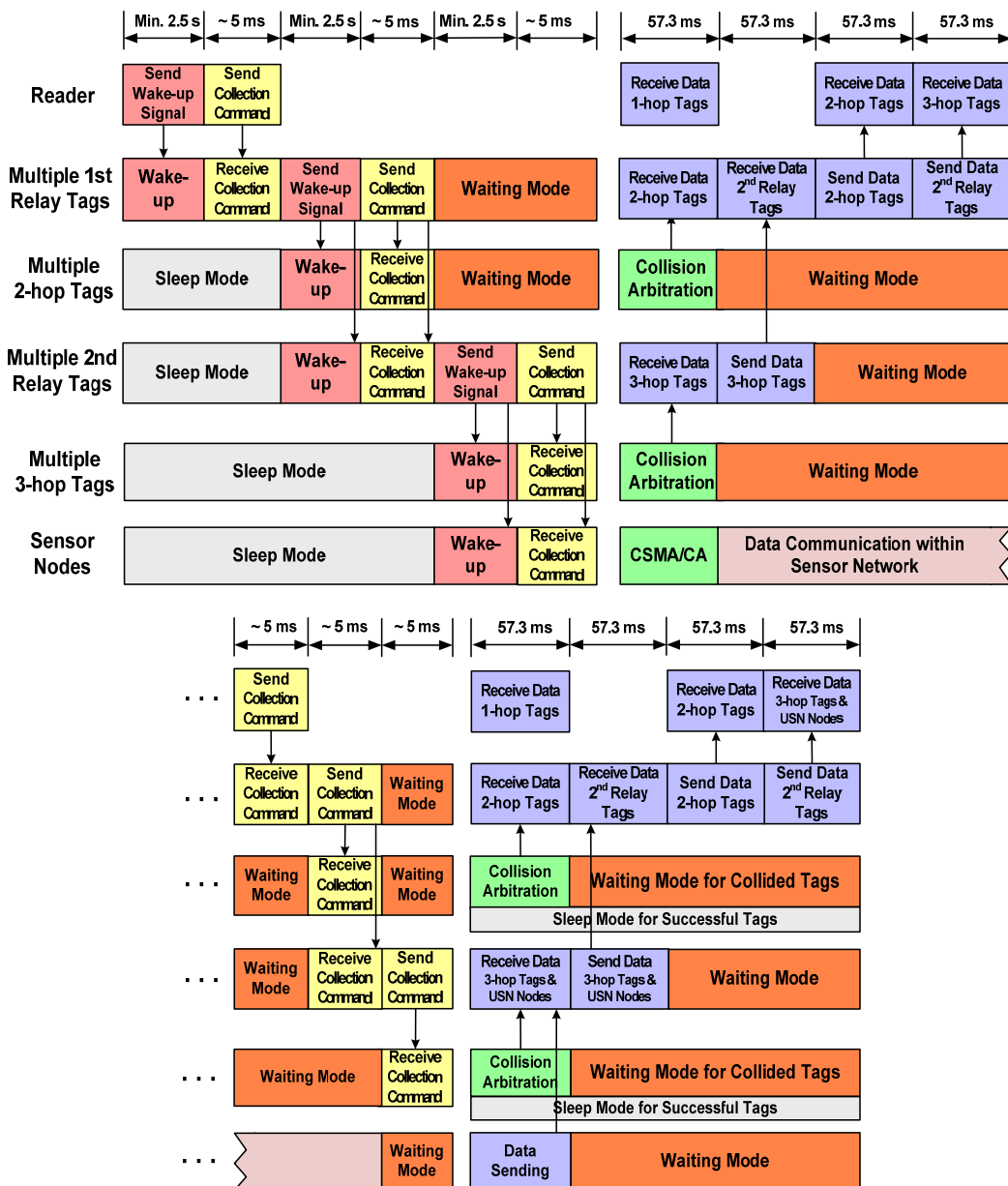

Fig. 5. Proposed frame structure of UWB based Class 4 RFID Multi-hop Relay System.

4. Simulation Results and Performance Analysis

For performance analysis, coverage and throughput are main performance metrics considered in the computer simulation.

The parameters used in the system level simulation (SLS) are listed in the **Table 3**, which refer to the proposals of Nanotron [14] for CSS and Sandlinks [15] for IR-UWB both compliant with IEEE 802.15.4a standards. We use the center frequencies 2.45GHz for CSS and 4GHz for IR-UWB with bandwidth 83.5 MHz and 500 MHz respectively. The transmission (Tx) power is 0 dBm and -14.3 dBm provided by Nanotron and Sandlinks, while the IEEE Task Group 4a (TG4a) defines a range of Tx power as -33 ~ 10 dBm for CSS and -41.3 ~ 0 dBm for IR-UWB. The total antenna gain and sensitivity are the same for both in order to reduce the effects of different devices. We compare the performances under both AWGN and CM1 channels.

Table 3. Parameters of CSS and IR-UWB for SLS

Parameters		Values	
		CSS	IR-UWB
Center Frequency		2.45 GHz	4 GHz
Frequency Band		83.5 MHz	500 MHz
Tx Power		0 dBm	-14.3 dBm
Tx & Rx Antenna Gain		0 dBi	0 dBi
Sensitivity		-94.5 dBm	-94.5 dBm
Pathloss (dB)	AWGN	$PL=40.2+20\log_{10}(d)$	$PL=44.48+20\log_{10}(d)$
	SV-model (CM1)	$PL=43.9+17.9\log_{10}(d)$	$PL=45.3+17.9\log_{10}(d)$
Shadowing (dB)	AWGN	Std. Dev. $\sigma_S = 3.7$, S = 1.4	
	SV-model(CM1)	(Shadowing) S = 2.2	
Coverage Target SNR for 10^{-3} BER(dB)		9.9 (AWGN) / 16.8(CM1)	9.8 (AWGN) / 11.5(CM1)
Data Rate		1 Mbps	0.87 Mbps

In system level simulation, we must consider the quality of service when we calculate the coverage. Hence, at first the target SNR for 10^{-3} BER of both CSS and IR-UWB is simulated based on the IEEE 802.15.4a PHY layer standards. **Fig. 6** shows the link level simulation of BER vs. SNR curves in AWGN and CM1 channels. The performances of CSS and IR-UWB are nearly the same under AWGN. However, compared both curves in CM1, the CSS curve is 5 dB worse than that of IR-UWB mainly due to the different coding scheme used in the simulation.

The data rate is 0.87 Mbps for IR-UWB, because we only consider $RS_6(63.55)$ encoding with coding rate 0.87 here in simulation and exclude the convolutional code.

4.1 Coverage Extension by UWB based Multi-hop Relay System

In the calculation of coverage, we simulate both IR-UWB and CSS under different channel models, AWGN and CM1 as **Fig. 7** and **Fig. 8** present. Note that the pathloss and shadowing are distinct. The sensitivity is another significant parameter for the practical realization and is hard to decide due to the hardware implementation. Here we give a range of the sensitivity from -90 dBm to -100 dBm. The equal power of the reader and relay tags is assumed.
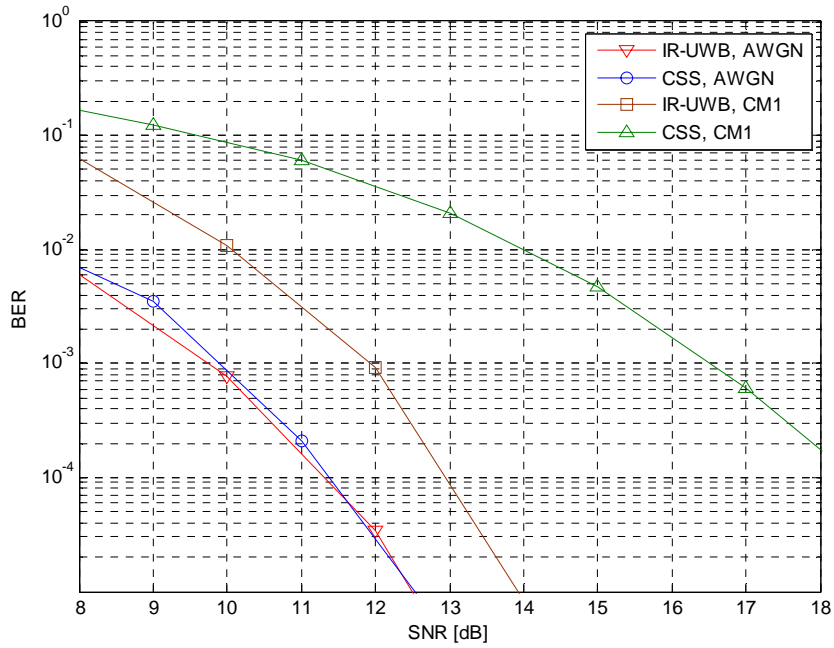
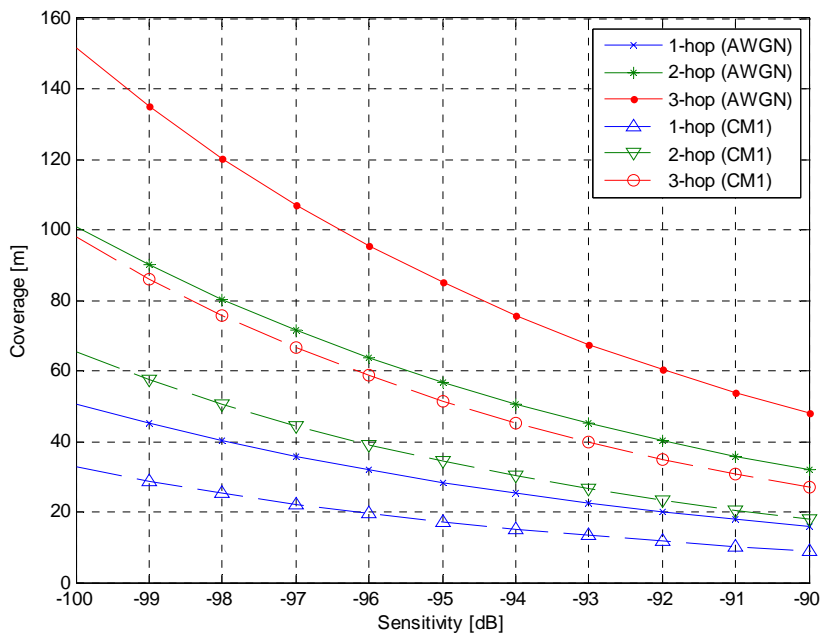**Fig. 6**. BER performacnes of IR-UWB and CSS in AWGN / CM1.
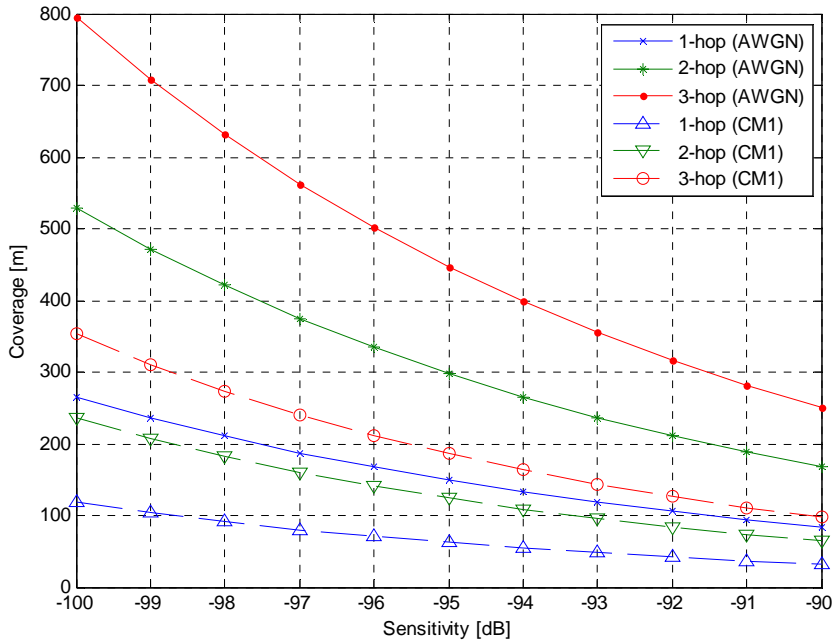

Fig. 7. Coverage of IR-UWB based RFID 3-hop system.

Fig. 8. Coverage of CSS based RFID 3-hop system.

Table 4. Coverage of 3-hop relay system with sensitivity of -94.5 dBm in CM1

Coverage (m)	IR-UWB		CSS	
Tx. Power (dBm)	0	-14.3	0	-14.3
1 Hop	106.65	17.165	61.97	9.721
2 Hop	213.3	34.33	123.9	19.442
3 Hop	319.95	51.494	185.9	29.163

4.2 Throughput Increasing by UWB based Multi-hop Relay System

For calculation of throughput, we assume the simulation model as **Fig. 9** shows.

A number of tags '*' are randomly distributed with a reader '□' in the center and 4 relay tags '○' within each hop. The coverage for each hop is obtained by the simulation results in CM1.

The expressions of throughput can be derived as [16]

$$
\begin{aligned}
\text{Throughput} &= \frac{\text{Total transmission bits}}{\text{Identification time}} \text{ (bps)} \\
&= \frac{\sum_i (\text{Transmission bits in the } i\text{-th successful slot})}{\text{Identification time}} \\
&= \frac{\text{Data rate} \times \sum_i (i\text{-th successful slot})}{\text{Identification time}} \\
&= \text{Data rate} \times \frac{\text{Total successful slot time}}{\text{Identification time}}
\end{aligned}
\tag{7}
$$

where the *identification time* is defined as the time to identify all the tags in the interrogation zone. Instead, we can use the total number of slots to reflect this performance. We assume that there are 200 slots in a frame and maximum 1000 tags deployed in the coverage of 3-hop relay system.
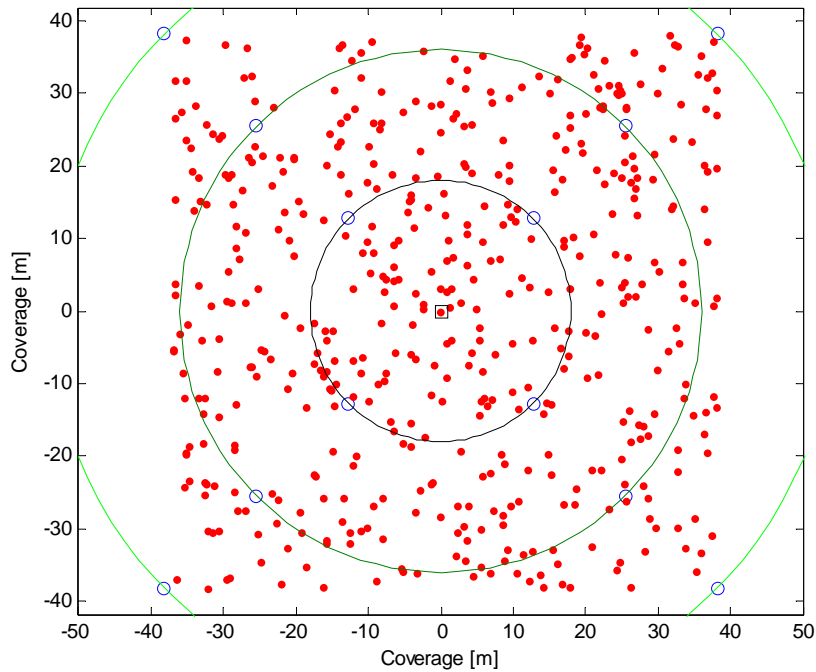

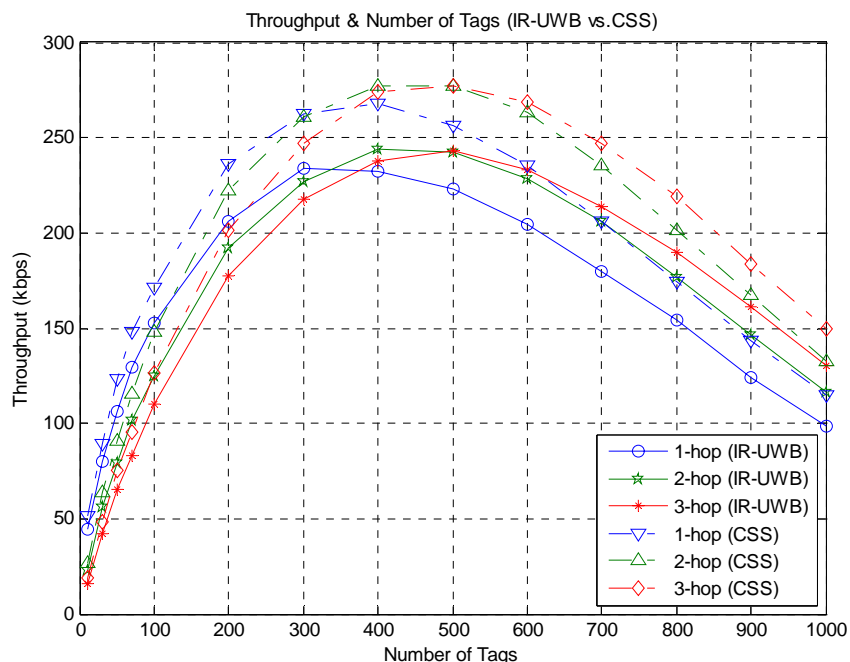**Fig. 9**. 500 tags are randomly distributed in active RFID 3-hop system.

Fig. 10. Throughput comparisons of IR-UWB and CSS with number of tags.

The throughput comparison of both two LR-UWB techniques defined in IEEE 802.15.4a PHY specification: IR-UWB and CSS are present in **Fig. 10**. We discern that the throughput is declining after it reaches a distinct peak value for each hop due to the catastrophic collisions.

In the SLS, CSS has a better throughput (277.1 kbps) than that of IR-UWB (244.4 kbps) with 500 tags for 3-hop relay system in **Table 5**. We notice that the throughput is going up with the adoption of multi-hop relay system. Also, the multi-hop relay system can load an increasing number of tags.

Table 5. Throughput of IR-UWB and CSS within 3 hops

Hop	Throughput	
	IR-UWB	**CSS**
1 Hop	268.1 (300 Tags)	233.9 (300 Tags)
2 Hop	276.9 (400 Tags)	244.2 (400 Tags)
3 Hop	277.1 (500 Tags)	244.4 (500 Tags)

5. Conclusions

In this paper, we proposed a new frame structure of active RFID multi-hop relay system based on ISO/IEC 18000-7 standard integrating with IEEE 802.15.4a PHY layer specification, which makes a connection with nearby USNs. In order to verify the improvements of the proposed frame structure, we simulate both IR-UWB and CSS PHY layers compliant with the specification to obtain the BER at target SNR. Also, we analyze the performances of our proposed multi-hop relay system, and the SLS results show that the coverage and throughput will be remarkably enhanced due to the adoption of multi-hop relay system. IR-UWB is undoubtedly a better choice with larger coverage than that of CSS given the same power. Also the throughput of both IR-UWB and CSS can be significantly enhanced. And the proposed active RFID multi-hop relay system enables to deploy a larger number of tags in the coverage of each hop.

References

[1] D. W. Engels and S. E. Sarma. "Standardization requirements within the RFID class structure framework," Technical Report, Auto-ID Center, Jan. 2005.

[2] ISO/IEC JTC 1, Information technology – Radio-frequency identification for item management – Part 7: Parameters for air interface communication at 433 MHz, ISO/IEC FDIS 18000-7:2004(E), May 2004.

[3] S. Hong, H. Zhang and K. Chang, "ISO/IEC 18000-7 based on RFID multi-hop relay system," in Proc. IEEE International Symposium on Communication and Information Technology (ISCIT), Sep. 2009.

[4] IEEE Standard 802.15.4a, IEEE Standard for Information technology - Telecommunications and information exchange between systems - Local and metropolitan area networks - Specific requirements, Part 15.4: Wireless medium access control (MAC) and physical layer (PHY) specifications for low-rate wireless personal area networks (LR-WPANs), Mar. 2007.

[5] M. Z. Win and R. A. Scholtz, "Impulse radio: how it works," IEEE Communication Letters, vol. 2, pp. 51-53, Feb. 1998.

[6] M. Z. Win and R. A. Scholtz, "Ultra-wide bandwidth time-hopping spread-spectrum impulse radio for wireless-access communicaitons," IEEE Trans. Commun., vol. 48, pp. 679-691, Apr. 2000.

[7]   B. Hu and N. C. Beaulieu, "Accurate evaluation of multiple-access performance in TH-PPM and TH-BPSK UWB systems," IEEE Trans. Commun., vol. 52, pp. 1758-1766, Oct. 2004.

[8]   M. Flury, R. Merz, J.-Y. Le Boudec, and J. Zory, "Performance evaluation of an IEEE 802.15.4a physical layer with energy detection and multi-user interference," in *Proc. IEEE Intl. Conf. Ultra-Wideband (ICUWB)*, pp. 663-668, Sep. 2007.

[9]   Z. Ahmadian and L. Lampe, "Performance analysis of the IEEE 802.15.4a UWB system," IEEE Trans. Commun., vol. 57, pp. 1474-1485, May 2009.

[10] A. Springer, W. Gugler, M. Huemer, L. Reindl, C.C.W. Ruppel, and R. Weigel, "Spread Spectrum Communications Using Chirp Signals," *EUROCOMM 2000, Information Systems for Enhanced Public Safety and Security*, pp. 166-170, 2000.

[11] A. F. Molisch, B. Kannan, C.-C. Chong, S. Emami, A. Fort, J. Karedal, J. Kunisch, H. Schantz, U. Schuster, and K. Siwiak, "IEEE 802.15.4a Channel Model-Final Report," *IEEE 802.15-04-0662-00-004a*, 2005.

[12] A. Goldsmith, "Wireless Communications," *Cambridge University Press*, 2005.

[13] Xin Wang and Georgios B. Giannakis, "CSMA/CCA: a modified CSMA/CA protocol mitigating the fairness problem for IEEE 802.11 DCF," *EURASIP Journal on Wireless Communications and Networking*, vol. 2006, pp. 1-12, Dec. 2005

[14] Nanotron Technologies, "Chirp Spread Spectrum (CSS) PHY presentation for 802.15.4a," http://www.ieee802.org/15/pub/05/15-05-0002-00-004a-nanotron-chirp-spread-spectrum-css-phy-presentation.ppt, Jan. 2005.

[15] Sandlinks, "Low-rate UWB alternate physical layer proposal submission for TG 802.15.4a," http://grouper.ieee.org/groups/802/15/pub/2005/15-05-0052-00-004a-symbol-interleaved-impulse-radio-cfp-presentation.ppt, Jan, 2005.

[16] X. Fan, I. Song, K. Chang, D.-B. Shin, H.-S. Lee, C.-S. Pyo, and J.-S. Chae, "Gen2-based tag anti-collision algorithms using Chebyshev's inequality and adjustable frame size," *Electronic and Telecommunication Research Institute (ETRI) Journal*, vol. 30, no. 5, pp. 653-662, Oct. 2008.

Hong Zhang received the BS degree in computer science from Jilin University, China, in 2007. After one year working experience in the industry, he is currently with The Graduate School of Information Technology and Telecommunications, Inha University, Korea, where he has been a MS student since 2008. His research interests include RFID/USN, reader/tag anti-collision MAC protocols, and UWB.

SungHyun Hong received the BS and MS degree in electronics engineering from Inha University, Incheon, Korea, in 2008 and 2010, respectively. His research interests include RFID/USN, reader/tag anti-collision MAC protocols, UWB.

KyungHi Chang received the BS and MS degrees in electronics engineering from Yonsei University, Seoul, Korea, in 1985 and 1987, respectively. He received his Ph.D. degree in electrical engineering from Texas A&M University, College Station, Texas, USA in 1992. From 1989 to 1990, he was with the Samsung Advanced Institute of Technology (SAIT) as a Member of Research Staff and was involved in digital signal processing system design. From 1992 to 2003, he was with the Electronics and Telecommunications Research Institute (ETRI) as a Principal Member of Technical Staff. During this period, he led the design teams of WCDMA UE modem and 4G radio transmission technology (RTT). He is currently with The Graduate School of Information Technology and Telecommunications, Inha University, where he has been an Associate Professor since 2003. His current research interests include RTT design for IMT-Advanced & 3GPP LTE systems, WMAN system design, cognitive radio, cross-layer design, cooperative relaying system, RFID/USN, and mobile ad-hoc network. Dr. Chang has served as a Senior Member of IEEE since 1998. Currently he is an Editor in Chief for the Korean Institute of Communication Sciences (KICS) Journal. He has also served as an Editor of ITU-R TG8/1 IMT.MOD, and he is currently an International IT Standardization Expert of Telecommunications Technology Association (TTA).